Segment based Detection and Quantification of Kidney Stones and its Symmetric Analysis using Texture Properties based on Logical Operators with Ultra Sound Scanning

R. Anjit Raja
Assistant Professor, Department of Computer Applications, Dr.Sivanthi Aditanar College of Engineering, Tiruchendur, TamilNadu, India.

J.Jennifer Ranjani, Ph.D
Associate Professor, Department of Computer Science and Engineering, Vivekanandha College of Engineering for Women, Tiruchengode, Namakkal, Tamilnadu,India.

ABSTRACT
In this research work a fully automated and given to automatic algorithm to detect Quantification of Kidney Stones by using symmetric analysis, which is proposed in this paper. Here we detect the renal-stones, segment the renal regions and calculate the area of the renal which is occupied by kidney stones. The quantitative analysis of kidney stones allows obtaining useful key indicators of disease progression. The stone detection is often an essential preliminary phase to solve the segmentation problem successfully. Thus, the user eventually notices that it is hard to detect the boundary of the kidney in the US image; even it's done by the trained sonographers. In addition, human error might occur during the interpretation of ultrasound image by untrained sonographer, especially when taking measurement. Therefore, in order to reduce the dependability to the sonographers' expertise, some image processing can be done which can automatically detect the centroid of human kidney and stones. Ultra Sound (US) is one of the modality of first choice in kidney image processing. US can be used to measure the size and appearance of the kidneys and to detect stones, congenital anomalies, swelling and blockage of urine flow. As this imaging technique is non-invasive, portable, and affordable and does not require radiation, most of the medical practitioner chosen US for primary screening of kidneys' condition. Three kinds of Ultrasound kidney images namely, Normal (NR), Medical Renal Diseases (MRD) and Cortical Cysts (CC) images are classified based on texture properties. This algorithm involves only convolution and simple arithmetic in various stages which leads faster implementation. The efficient feature space is created for textures as well as US kidney stone classification.

Firstly, some techniques of speckle noise reduction were implemented consist of median filter, Wiener filter and Gaussian low-pass filter. Then texture analysis was performed by calculating the local entropy of the image, continued with the threshold selection, morphological operations, object windowing, determination of seed point and ROI generation. This method was performed to several kidney ultrasound images with different speckle noise reduction techniques and different threshold value selection. Based on the result, it shows that for median filter, threshold value of 0.6 gave the highest TRUE ROIs which were 70%. For Wiener filter, threshold value of 0.8 gave highest TRUE ROIs which were 80% and for Gaussian low-pass filter, threshold value of 0.7 gave highest TRUE ROIs which were 100%. By using the previous methods result, this method has been tested also to more than 200 kidney stone ultrasound images. Therefore, we conducted a texture analysis to the kidney stone images. As the result, the renal sinus, the central area of the kidney stone appeared brighter compared to the other part of the renal, and in the texture analysis, it also appear as the most common region detected in kidney stones.

General Terms
Algorithm, kidney stones, segmentation, sonography, Medical Renal Diseases, Ultrasound, texture, threshold

Keywords
Ultrasound Image, Sonographer, Radiation, Morphological-Operations, Texture Analysis, Region of Interest

1. INTRODUCTION
Ultrasound has been a welcome tool for many years to break up kidney stones, but finding the stones still requires radiograph or CT imaging. The accurate diagnosis of a renal stone is dependent on many factors, including the clinical history, the nature of the imaging findings, the experience of the radiologist, and the quality of the examination. A high-quality imaging examination, which is under the control of the radiologist, is essential. We present our technique in the performance of US imaging for the evaluation of kidney stone range and acknowledge that other protocols work equally well. It is expected that these protocols will be modified over time as new equipment becomes available. Ultrasound has been shown to be relatively safe but no imaging method which deposits additional energy into the body should be considered entirely risk free. When the decision to make a diagnostic image is made, the physician should always make a conscious judgement about whether the potential benefits of the imaging procedure are greater than any potential risk. In recent years a great effort of the research in field of medical imaging was focused on kidney stone, renal cavity segmentation. The automatic segmentation has great potential in clinical medicine by freeing physicians from the burden of manual labeling;

whereas only a quantitative measurement allows to track and modeling precisely the kidney disease. Despite the undisputed

usefulness of automatic stone segmentation, this is not yet a widespread clinical practice, therefore the automatic kidney stone segmentation is still a widely studied research topic. The main difficulties in field of automatic stone-area segmentation are related to the fact that the renal stone are very heterogeneous in terms of shape, color, texture and position and they often deform other nearby anatomical structures. Normally the kidney diseases are classified as hereditary, congenital or acquired. The detection of calcifications inside the body is a large field of study including several dynamic areas of research, which is mainly useful for diagnosing the kidney stone diseases. The actual kidney stones may be rough non-spherical in shape, but the dominant effects that are used to find the Fracture in actual kidney stones, are based on the reverberation time across the length of the stone. Due to the presence of powerful speckle noise and attenuated artifacts in abdominal ultrasound images, the segmentation of stones from these images is very complex and challenging. Hence, this task is performed by the use of much prior information such as texture, shape, spatial location of organs and so on. Several automatic and semiautomatic methods have been proposed. Even though the performance such methods are better when the contrast-to-noise ratio is high, it deteriorates quickly when the structures are inadequately defined and have low contrast like the neuroanatomic structures, such as thalamus, globus pallidus, putamen, etc. If any modern techniques are implemented on the medical images it will be very helpful for the objective diagnosis. One such technique is the development of an algorithm using logical operator method to classify the image using its texture properties. Different regions of an image are identified based on texture properties [1]. Some of the applications that demonstrate the importance of texture analysis are found in medical images, remote sensing and industrial images. Textures are usually characterized by its features. Features are extracted based on logical operator to classify the image [2]. This technique is usually applied for medical images to enhance the quality of representation and better understanding of hidden information for proper objective diagnosis. In this project, the texture properties are applied to the medical images to classify the three different categories of Ultrasound kidney images. By using this technique, it is also possible to extract some features that will be very helpful for the diagnosis of the medical images to make comparative study on images for better decision making. This method gives an excellent performance on texture images. So it can be applied to the medical US kidney stone image classification and compare the performance with the texture result.

2. RELATED WORK

There were some previous researches done in exploring the semi-automatic and automatic ultrasound scanning especially in breast imaging. Sinha et al. developed an automated ultrasound imaging-mammography system where a digital mammography unit has been augmented with a motorized ultrasound transducer carriage above a special compression paddle. Yap et al developed a novel algorithm for initial lesion detection in ultrasound breast images which automatically generate region of interest (ROI) in exchanged of manually cropped ROIs. For this paper, we have developed a new technique that automatically detects the kidney stone's centroid in kidney stone US videos, which were separated into single frame images first. This study consists of the use of few filtering techniques for speckle noise reduction and image enhancement as well as texture analysis in analyzing the kidney structure in US images. The technique is helpful in recognizing the kidney in an image, which will help the sonographers in confirming the detection of the kidney as the detected kidney stone can be an indicator for correct scanning rules. Besides, this study also can help untrained sonographer to improve their skills in US scanning.The rest of this paper is organized as follows. In section 3, we describe on the materials and the procedure of image acquisition and the detection procedure of the centroid of the kidney stone in ultrasound video. Image segmentation [3] represents a method of separation a portion of image into separate area. A great assortment of dissimilar segmentation approaches for images have been developed. The Segmentation of an image entails the division or separation of the image into regions of similar attribute. The ultimate aim in a large number of image processing applications is to extract important features from the image data, from which a description, interpretation, or understanding of the scene can be provided by the machine. This paper illustrate segmentation scheme consists of two stages. In the *opening stages*, the US kidney stone image is obtained from image-frame database, which is converted from the form of US Video to single frames. In that frame artifact and noise are disconnected. In the *subsequent stages* (US) image segmentation is to precisely recognize the major renal arrangement in these image areas.

After getting the correctly arranged renal areas, we can perform the following operational steps,

- The input image sample is convolved with six different types of operators.
- The standard deviation matrix is computed on the convolution response.
- Zonal filtering masks are applied to the standard deviation matrices and features are computed.
- A classifier is used to identify the unknown sample from the reduced feature space.

2.1. General Texture Image Classifications

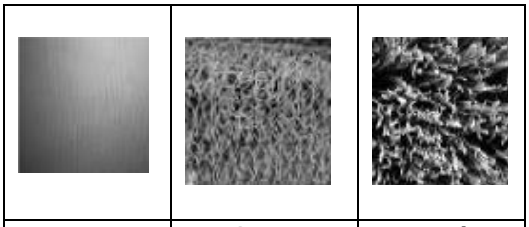

Fine	Coarse	Rough

2.2. US Kidney Images Classifications

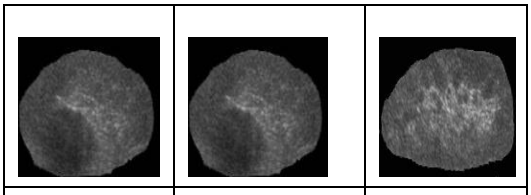

CC	MRD	NR

2.2.1 Logical Operators

In this paper, six types of operators are used for texture classification [4]. All the operators are of size 2 x 2, which is adequate in generating an efficient feature space. Hence, the

logical operator considered here are order-2 elementary matrices. The building blocks for defining these matrices are 0, 1,-1, matrices of order 1 x 1. The order-2 matrices are generated by using row-wise joins (RWJ) and column-wise join (CWJ) on these basic building blocks. When the RWJ operation is applied to the above order 1 x 1 matrices for all possible concatenation, there are nine different matrices of order 2 x 1, which are shown in Fig 1.

$$\begin{bmatrix}1\\1\end{bmatrix}\begin{bmatrix}1\\-1\end{bmatrix}\begin{bmatrix}-1\\1\end{bmatrix}\begin{bmatrix}-1\\-1\end{bmatrix}\begin{bmatrix}1\\0\end{bmatrix}\begin{bmatrix}0\\1\end{bmatrix}\begin{bmatrix}0\\-1\end{bmatrix}\begin{bmatrix}-1\\0\end{bmatrix}\begin{bmatrix}0\\0\end{bmatrix}$$

Fig 1: Basic operator generation matrices

Then, the CWJ operation is applied to the above order 2 x 1 matrices for all possible concatenation, 81 different matrices of order 2x2, basic core matrices are shown in Fig.2. Only 2 x 2 is sufficient in transforming the textures in to an effective feature space. The higher order matrices are obtained by successive application of the Kronecker product to the core matrices shown in Fig 2. In this paper, six types of operators are used for texture classification. They are logical Hadamard, Arithmetic, Adding, equivalence, conjunction, and disjunction operators.

2.2.2 Logical hadamard Operator

The logical Hadamard Operator is nothing but the Walsh Hadamard transform. Walsh functions and transforms are important analytical tools for signal processing and have wide applications in digital communications, digital image processing as well as digital logic design [5]. To build this transform is very simple compare to other transforms.

2.2.3 Arithmetic Operator

In many applications of arithmetic operator, the values of only some spectral coefficients are needed. An efficient way has been developed for calculating the transform, which has the ability to evaluate only some chosen spectral coefficients.

2.2.4 Adding Operator

Just like Arithmetic operator, Adding operator can be chosen.

1 1 1 -1	1 0 1 1	1 0 -1 1
O1:Hadamard	**O2: Adding**	**O3:Arithmetic**
1 0 0 1	0 0 0 1	0 1 1 1
O4: Equivalence	**O5: Conjunction**	**O6: Disjunction**

Fig 2: Basic core operators for texture classification

i. Equivalence Operator"<=>": The equivalence operator is true if *x* and *y* have identical values.

ii. Conjunction Operator "^": The conjunction of *x* and *y*, *x* ^ *y*, is true if *x* and *y* are both true and is false otherwise. This operation same as the "AND" operation.

Disjunction Operator "v": The disjunction of *x* and *y*, *x* v *y*, is false if *x* and *y* are both false and is true otherwise. This operation same as the "OR" operation.

Table 1: Equivalence, Conjunction, and Disjunction Operations

x	y	x <=> y	x ^ y	x v y
F	F	T	F	F
F	T	F	F	T
T	F	F	F	T
T	T	T	T	T

3. MATERIALS AND METHODS

For this study, longitudinal and transverse view of ultrasound kidney images were taken from volunteers from University Technology Malaysia Johor Bahru- (UTM) by using TOSHIBA *AplioMX* ultrasound machine with 3.5MHz transducer. The kidneys were scanned in supine position where the subjects were lying down with the face upward and with inspiration of the subjects.

Fig 3: Longitudinal section of original ultrasound kidney - image

Fig 4: Transverse section of original ultrasound kidney-image

To develop the system for generating the kidney ultrasound region of interest automatically. Fig. 3 shows the longitudinal section of the original ultrasound kidney image while Fig. 4 shows the transverse section of the image. As explained earlier, the kidney image for longitudinal view is in football shaped and the image for transverse view is C shaped. For this kind of process, an automatic defined rectangular ROI will be generated and this ROI generation can be used as a preprocessing step for any other segmentation method since it only cuts the redundant background while keeping the kidney and renal stones. Fig. 5 shows the block diagram of the steps for ROI generation. Firstly, the speckle noise reductions were performed. For this study, three speckle noise reduction techniques were chosen to be compared consist of median

filter, Wiener filter and Gaussian low-pass filter. In order to choose the best filter which helps in optimizing the generation of ROI for kidney stone US images, comparisons were made between those filters by evaluating their performance in detecting the most ROIs after being tested with several kidney US images. Then texture analysis [6] is implemented for creating texture image and based on the threshold value selected, morphological operation is used for removing unwanted regions.

After that, the remaining objects will be windowed so that only one object is chosen as the seed point.

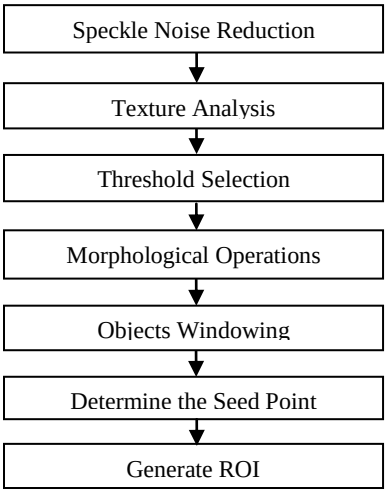

Fig 5: Block diagram for ROI generation

Lastly, the ROI is generated according to the seed values.

4. PROPOSED KIDNEY STONE SEGMENTATION TECHNIQUE

The proposed renal kidney stone segmentation method consists of five major steps namely, (i) Determining inner region indicators (ii) Determining the region parameters (iii) Enhancing the contrast of the image using Histogram Equalization (iv) Finding most fascinated Pixels by K-means clustering [7] and (v) Contour based Region selection process. The proposed kidney stone segmentation training and testing procedure is shown in Figure 6.

4.1 Preprocessing

In this preprocessing phase, principal component analysis with local pixel grouping (LPG-PCA) based image denoising algorithm is used to remove the noise from the US renal calculi images.

4.2 Determining Inner Region Indicators

Let D represents the renal calculi image training dataset, which contains renal calculi images D = {I1, I2 ,…In};n = 1…N, where *N* is the number of the renal calculi images in the given dataset D . To determine the inner region indicators, Then the whole image is divided into *L* number of blocks and for every block, an index value, firstly, the regions representing kidney are manually marked in the known training data set ultrasound i mages [8].

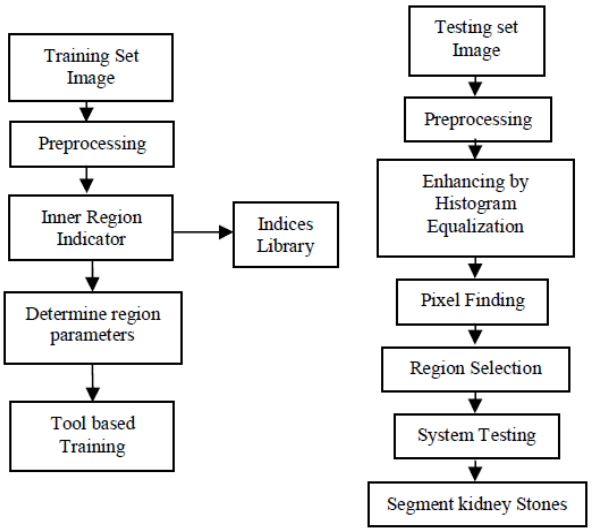

Fig 6: Proposed KSST segmentation training and testing-procedure

which can be represented as $i\ B = \{ I\} : i = 1 \ldots L$, is allocated. Then, each block included in *B* is checked to find the edge pixels present in the kidney [9]. If any block is found to be containing edge pixels of the kidney, then the index value of the corresponding block is kept as $l\ K = \{I\} : l \in L$. Hence, *K* which can also be called as indices library, contains the indices of blocks of all the known images.

4.3 Determine Region Parameters

Using the renal calculi images in D, the calculi and non calculi regions are extracted. The extracted regions from the renal calculi images are R = {r1, r2 ,….r_m},m = 1…M, where M Represents the total number of extracted regions. Next we find the centroids values for all the renal part of images in D, that is $C(x,y) = \{c_1^{I_1}(x,y), c_2^{I_2}(x,y), \cdots c_n^{I_n}(x,y)\}$, where $c_1^{I_1}(x,y)$ is a centroid value of image I1. Then, we determine the region parameters for the extracted regions from R by utilizing MATLAB function. The region parameters determined for each region are (i) Area (ii) Centroid (iii) Orientation and (iv) Bounding Box. This region parameter values are given to the ANFIS system for training process. In training process, the normal and calculi area is identified by the threshold values t_1 and t_2. The ANFIS system result value is represented as χ.

The final decision is defined by

$$\chi = \begin{cases} t_1 == \text{normal} \\ t_2 == \text{calculi} \end{cases} \quad (1)$$

4.4 Contrast Enhancement using Histogram Equalization

In contrast to the following enhancement process, initially we have converted given ultrasound image t_n I into a grayscale image $\mathbf{G^{t'}_n}$, as histogram equalization process can be used only on grayscale -images. Histogram equalization [10] make some enhancements to the contrast of the given gray scale ultra sound image. In histogram equalization all pixel values in gray scale image are adjusted to maximum intensity values of the image. The mage that is obtained after the histogram equalization process is denoted as $\mathbf{G^{t'}_n}$.

4.5 Find Most Fascinated Pixels by K-means clustering

Mostly required pixels are computed from the image $\mathbf{G^{t'}_n}$ by utilizing the k-means clustering method. K-means clustering is a method of cluster analysis which aims on partition of observations into number of clusters in which each observation belongs to the cluster with the nearest mean. The steps involved in the K-means clustering used in our method are described as following:-

(i) Partition of the gray scale data points to A arbitrary centroids, one for each cluster.
(ii) To determine new cluster centroid by calculating the mean values of all the cluster elements.
(iii) Determining distance between the cluster centroid and the cluster elements and obtain new clusters.
(iv) Repeat process from step
(1) Till a defined number of iterations are performed.
The k-means algorithm aims at minimizing an objective function

$$H = \sum_{a=1}^{A} \sum_{g=1}^{G} \left\| d_g^a - C_a \right\|^2 \quad (2)$$

In eqn (2) $\mathbf{d^a_g}$ represents data points and Ca means center of the cluster. The resultant of the k-means clustering process has a number of clusters, which forms a cluster-enabled image IA [11]. Here we can select the cluster, with maximum white color pixel values, and is applied to the newly created mask I'.

4.6 Region Selection Process

Region selection process performed using renal calculi images are taken from the testing image dataset $D^t = \{I_1^t, I_2^t, \cdots I_n^t\}; n = 1 \cdots N^t$, where *N* represents the total number of renal calculi images in the dataset D^t [12]. The dataset D^t contains the images that are in the dimension of $P \times Q$; $1 \le p \le P$, $1 \le q \le Q$. To accomplish the region selection process, a contour extraction process is utilized.

4.6.1 Multidirectional Traversal

Here we have proposed two major traversals called bottom-up traversal and top-down traversal. In each of the traversal, a left-right traversal is applied. The traversals are applied over U, which is binary. At the time of two major traversals, once the pixel with '1' is obtained, then left-right traversal is enabled so that all the regions in the same axis and the region of the first obtained pixel are removed from the mask. The survived pixel values are marked into the original test image and it is subjected to the consequent process of thresholding [13].

4.6.2 Thresholding

Here, a chain of thresholding process is performed in the original image.

• Firstly, the pixel values that are marked by using the previous process are compared against a defined threshold value t_3. The pixel values those are greater than t_3 are stored in a newly created mask U_s.

• The region parameters are determined for the regions in the mask U_s and the computed region parameters are given to the ANFIS to obtain the ANFIS score. If the ANFIS score is greater as compared to t_4, then the selection of regions is performed.

• Then, we count the number of neighbor pixel values around the selected regions which are greater than the threshold value t_5, and the number of count value of each region is compared with the threshold value t_6. If the count value is greater than the threshold value t_6, then the regions are selected.

• The selected regions from the previous thresholding process are involved in the morphological dilation operation [14]. After the morphological operation, count the number of regions that are presented in the image. The region count value is compared with two threshold values t_7 and t_8.

• If the count value is greater than t_7, then perform the traversing down operation once, and if the count value is greater than t_8, then perform traversing down operation in multiple times.

• In the final thresholding process, each regions area value is calculated and it is compared with the threshold values t_9 and t_{10}. The regions that are less than t_9 and greater than t_{10} are selected. The selected regions are then placed into the original testing image $\mathbf{I^t_n}$.

By performing all the above described process in various renal calculi kidney images, the kidney stone region is segmented.

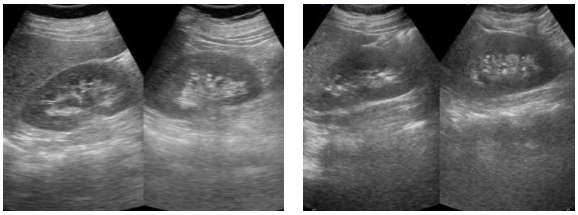

Fig 7: Normal Renal Image and Renal Image with kidney-stone

5. TEXTURE ANALYSIS

Texture analysis is important in characterizing regions in an image by their texture content and it is helpful when objects in an image are more characterized by their texture than by intensity, and traditional thresholding techniques cannot be used effectively [15]. When certain values either range, standard deviation or entropy of the image are calculated, they will provide information about the local variability of the intensity values of pixels in the image, thus the texture can be characterized. The toolbox in MATLAB includes three texture analysisfunctions that filter an image using standard statistical measures, such as range, standard deviation, and entropy. *Rangefilt* is used to calculate the local range of the image. If the image has smooth texture, it will have small value, whereas if the image's texture is rough, the value will be larger. *stdfilt* is used to calculate the local standard deviation of an image while *entropyfilt* is used to calculate the local entropy of a grayscale image which also represents a statistical measure of randomness. For this study, all three texture filters were applied to the kidney US images [16]. Then, threshold value is set to segment the textures. Threshold value of 0.7 is selected because it is roughly the intensity value of pixels along the boundary between the textures in US

kidney images. Depending on the result for texture filtering, only the best filter is chosen to be applied to the rest of kidney US images.

5.1 Determine the Seed Point

The left regions will undergo another selection steps to determine which is the correct seed point. The algorithm for seed point selection is as in Fig.8

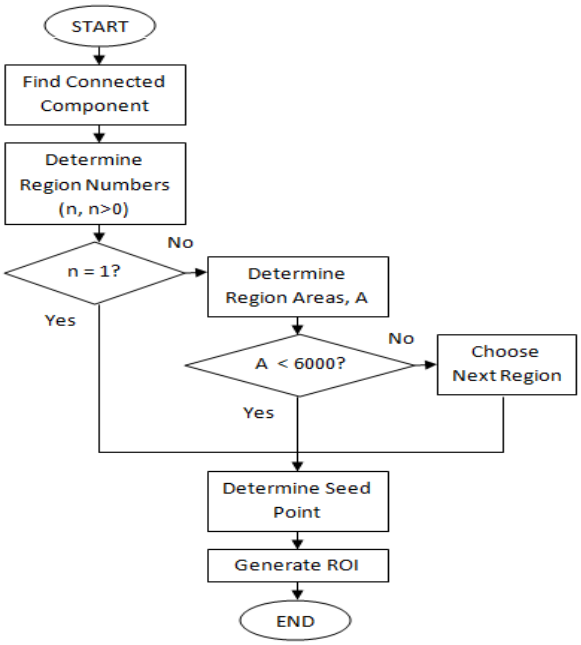

Fig 8: Algorithm for seed point detection

For seed point detection, firstly, the number of connected components (region), n needs to be determined so that we can know how many regions left in the image [17] . If there is only one region left, it is automatically considered as the seed point. If not, the region areas (pixel), A also needs to be determined. We set the threshold pixel areas as 6000. If the area, A is less than 6000, that region is selected as the seed point. If not, the other region will be selected. Then, the center pixel value (x, y) of the winning region is determined and based on the value, a rectangular window is defined to generate longitudinal and cross section ROI of kidney [18]. For longitudinal kidney image, a window of 400x200 is defined and for transverse kidney image, a window of 240x240 is defined. The algorithm was tested for more than 200 images and the results were displayed in Fig.9

Fig 9: Multiple, small kidney stones

This elderly male patient has a history of stone disease. But the most striking feature of the ultrasonography of the kidneys in this patient (see ultrasound images above), is not the solitary large calculus (19 mm.) in the right kidney, but the multiple small stones distributed throughout the calyces of both kidneys [19]. These numerous kidney stones measured from 2 to 4 mm. in size and number more than 10 per kidney. Such appearances can mimic the renal conditions like nephrocalcinosis and medullary sponge kidneys. But medullary sponge kidneys usually produces a bunch of grapes appearance for the calculi.

Fig 10: Image with Calculus

Finally, the selected regions from the thresholding process are given to the original image that is demonstrated in the following figure 11. In figure 11, the calculi regions are exactly marked in red color. The result image has shown that the proposed segmentation method has exactly found the calculi -region from the renal calculi images. The performance of proposed segmentation method [20] is analyzed with different images and it is described in the following section.

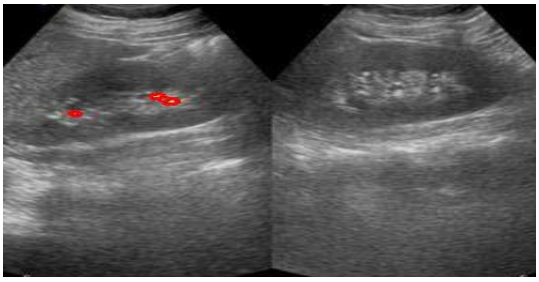

Fig 11: Proposed Segmentation Result Image

6. RESULT ANALYSIS

The performance of the segmentation method by using four testing images is given in table 2. This performance analysis exploits statistical measures, to compute the accuracy of calculi segmentation done by the segmentation method. The performance of the segmentation analysis is shown in the below table 2.

Table 2: Statistical performance measures for four different US renal calculi In Table 2.

Is No	Se	Sp	Acc	FPR
1	92.22	98.95	98.94	0.07
2	86.03	100	98.97	0
3	100	100	100	0
4	100	100	100	0
Average	94.60	99.74	99.48	0.02
Is No	**PPV**	**NPV**	**FDR**	**MCC**

1	59.96	99.99	40.04	74.77
2	100	99.98	0	94.36
3	100	100	0	100
4	100	100	0	100
Average	89.99	99.99	10.01	92.28

We have achieved high sensitivity, specificity and accuracy level in 1 sec computational time. The segmented stone area by segmentation method is using conventional segmentation algorithms [21]. A relative error is calculated between the segmented stone area marked by the expert radiologist and the proposed method. The formula for the calculation of relative error is described in eqn. 3,

$$\nu = \left| \frac{E - P}{E} \right| \times 100 \quad (3)$$

Where, ν - Relative Error E - Stone area marked by Expert radiologist P - Stone area marked by the proposed segmentation method the stone area marked by the expert radiologist, the segmentation method and its relative error are given in Table 3. The computational time of the method is obtained from the calculi detection process [22]. The average computational time of the system is shown in the Table 4 for four renal calculi images. The computational time of this method is very low.

Table 3: segmentation relative error performance

Radiologist expert (mm^2)	Kidney Stone Area(mm^2)	Error of this Method
88.5	88.4	0.01
61.6	61.7	0.16
64.0	64.1	0.01
91.8	90.2	1.06
72.0	72.1	0.00
24.9	24.8	0.01
120.1	120.0	0.01
35.0	35.0	0.00

Table 4: Computational time of the Segmentation Methods

Systems	Images	Computational Time(Sec)
	1	1.243566
	2	1.423456
	3	1.653336
	4	1.534332
	Average	1.4636725

7. CONCLUSION

In this paper, a KSST segmentation method to segment the calculi from the renal calculi images was proposed. The proposed method was implemented and set of renal calculi images were utilized to evaluate the proposed KSST segmentation method. The proposed method has exactly detected the calculi and produced a high segmentation accuracy result. The performance of segmentation method was analyzed has produced less relative error. Moreover, our proposed KSST segmentation method has produced 99.74% of accuracy, 94.60% sensitivity and 99.48 % specificity values. For further research, improvement can be made by selecting another better filter, as well as by investigation the morphological operation in finding the optimum values for detecting more accurate kidney stones.

8. ACKNOWLEDGMENTS

Our sincere thanks go to head of institution and principal of our colleges and our departments head.

9. REFERENCES

[1] P. P. Raghu and B. Yegnanarayana, “Segmentation of Gabor filtered textures using deterministic relaxation”, IEEE Trans. Image Process, vol. 5, no. 12, (1996), pp. 1625-1636.

[2] M. Varma and A. Zisserman, “Classifying images of materials: Achieving viewpoint and illumination independence”, Proceedings of the 7th European Conference on Computer Vision, vol. 3, (2002), pp. 255-271.

[3] A. Madabhushi, N. Dimitris, Mctaxas, “Combining low-high-level and empirical domain knowledge for automated segmentation of ultrasonic breast lesions”, in IEEE Trans. On Medical Imaging, vol. 22, no. 2, 2003, pp. 155-169.

[4] O. G. Cula and K. J. Dana, “3D texture recognition using bidirectional feature histograms”, Int. J. Comput. Vis., vol. 59, (2004), pp. 33-60.

[5] C. Schmid, “Weakly supervised learning of visual models and its application to content-based retrieval”, Int. J. Comput. Vis., vol. 56, (2004), pp. 7-16.

[6] M. Varma and A. Zisserman, “A statistical approach to texture classification from single images”, Int. J. Comput. Vis., vol. 62, (2005), pp. 61-81.

[7] B. Caputo, E. Hayman and P. Mallikarjuna, “Class-specific material categorization”, Proceedings of the International Conference on Computer Vision, vol. 2, (2005), pp. 1597-1604.

[8] Yap, M.H., Ewe, H.T., Region of interest (ROI) detection in ultrasound breast images. In: Proceedings of MMU International Symposium on Information and Communications Technologies (M2USIC). Cyberjaya, Malaysia: Multimedia University; 2005: 5–8.

[9] M. M. Fernandes, C. A. Lopez, “An approach for contour detection of human kidneys from ultrasound images using Markov random fields and active contour”, in Medical Image Analysis. 2005. 9: pp. 1-23.

[10] Bommanna Raja, Madheswaran and Thyagarajah,"A General Segmentation Scheme for Contouring Kidney Region in Ultrasound Kidney Images using Improved Higher Order Spline Interpolation",International Journal of Biological and Life Sciences, Vol. 2, No. 2, pp. 81-88, 2006.

[11] Neil R. Owen, Oleg A. Sapozhnikov, Michael R.Bailey, Leonid Trusov and Lawrence A. Crum, "Use of acoustic -scattering to monitor kidney stone fragmentation during shock wave lithotripsy", In Proceedings of IEEE International Ultrasonics Symposium, Vancouver, Canada, pp. 736-739, 2006

[12] C. H. Wu, Y. N. Sun, "Segmentation of kidney from ultrasound B-mode images using texture-based classification", in Computer Methods and Programs in Biomedicine, 2006, 84: pp. 117-123.

[13] S. P. Sinha, M. M. Goodsitt, M. A. Roubidoux, R. C. Booi, G. L. LeCarpentier, C. R. Lashbrook, K.E. Thomenius, C. L. Chalek, P. L. Carson, "Automated Ultrasound Scanning on a Dual-Modality Breast Imaging System Coverage and Motion Issues and Solutions", in Journal of Ultrasound in Medicine, vol. 26, no. 5, 2007, pp. 645-655.

[14] M. H. Yap, E. A. Edirisinghe, H. E. Bez, "A novel algorithm for initial lesion detection in ultrasound breast images", in Journal of Applied Clinical Medical Physics, vol 9, no 4, 2008.

[15] Yap, M.H., Edirisinghe, E.A., Bez, H.E., A novel algorithm for initial lesion detection in ultrasound breast images, Journal of Applied Clinical Medical Physics, Volume 9, Number 4, 2008.

[16] Cheng, H.D., Shan, J., Ju, W., Guo, Y., and Zhang, L., Automated breast cancer detection and classification using ultrasound images: A survey, Pattern Recognition 43, 1 (2010), 299-317.

[17] Hafizah, W.M., Supriyanto, E., Comparative Evaluation of Ultrasound Kidney Image Enhancement Techniques, International Journal of Computer Applications, 2011, Volume 21, No. 7, pp.15-19.

[18] V. Shrimali, R. S. Anand, V. Kumar, "Comparing the performance of ultrasonic liver image enhancement techniques: a preference study", in IETE Journal of Research, vol 56, issue 1, 2010.

[19] Local binary pattern histogram based texton learning for texture classification, Yonggang He, Nong Sang and Rui Huan,18th IEEE Int.Conf.on image processing, (2011).

[20] Suprianto, E., Jamlos, M.A., Kheung, L.K., Segmentation of Carotid Artery Wall towards Early Detection of Alzheimer Disease,Proceedings of 15th WSEAS International Conference on Computers, 2011, pp.201-206.

[21] Suprianto, E., Hafizah, W.M., Wong, W.Y., Ultrasound Pancreas Segmentation: A New Approach Towards Detection of Diabetes Mellitus, Proceedings of 15th WSEAS International Conference on Computers, 2011, pp.184-188.

[22] U Ravi Babu , "Texture Classification Based on Texton Features",IJ I GSP,vol. 8, (2012), pp. 36-42.